Immunity & Ageing

RESEARCH

Open Access

Quercetin ameliorates lupus symptoms by promoting the apoptosis of senescent Tfh cells via the Bcl-2 pathway

Feng Xiong[1†], Kai Shen[1†], Di Long[2], Suqing Zhou[1], Pinglang Ruan[1], Yue Xin[1], Yuezheng Xiao[1], Weijun Peng[3], Ming Yang[1*], Haijing Wu[1*] and Qianjin Lu[1,4,5,6*]

Abstract

Systemic lupus erythematosus (SLE) is an autoimmune disorder that commonly affects the skin, kidneys, joints, and various other systemic tissues, with its development intricately linked to the process of immunosenescence. Quercetin (QC), a phytochemical that occurs naturally, demonstrates many different biological capabilities, such as antibacterial, antioxidant, and anti-inflammatory activities. Our investigation found that QC effectively reduced kidney damage and relieved mesenteric lymph nodes (mLNs) swelling in MRL/lpr lupus mice. Moreover, QC has been found to decrease the number of senescent follicular helper T (Tfh) cells, a pivotal kind of T cells that contribute to the progression of SLE. In vitro, QC exhibited the capacity to modulate mRNA expression levels, with the downregulation of *IL-6*, *IL21-AS1*, *IL-27*, *BCL6*, and *BCL2L12*, and the upregulation of *FOXP1* and *BIM*. This modulation resulted in the suppression of Tfh cells differentiation and the enhancement of apoptosis in senescent $CD4^+$ T cells. In addition, the HuProtTM Human Proteome Microarray revealed that QC can directly bind to BCL-2 protein and therefore promote the apoptosis of senescent $CD4^+$ T cell. As a result, our investigative elucidate the potent inhibitory action of QC on the ontogeny of Tfh cells, along with its capacity to abrogate the immunosenescent phenotype. This positions QC as a promising therapeutic strategy for treating SLE.

†Feng Xiong and Kai Shen contributed equally to this work.

*Correspondence:
Ming Yang
yangming_0216@csu.edu.cn
Haijing Wu
chriswu1010@csu.edu.cn
Qianjin Lu
qianlu5860@pumcderm.cams.cn
[1]Department of Dermatology, Hunan Key Laboratory of Medical Epigenomics, The Second Xiangya Hospital of Central South University, 139 Middle Renmin Road, Changsha, Hunan 410011, China
[2]Department of Dermatology, The Second Affiliated Hospital, Hunan University of Traditional Chinese Medicine, Changsha, China
[3]Department of Integrated Traditional Chinese and Western Medicine, The Second Xiangya Hospital, Central South University, Changsha, China
[4]Hospital for Skin Diseases, Institute of Dermatology, Chinese Academy of Medical Sciences & Peking Union Medical College, Nanjing 210042, China
[5]Key Laboratory of Basic and Translational Research on Immune-Mediated Skin Diseases, Chinese Academy of Medical Sciences, Nanjing, China
[6]Jiangsu Key Laboratory of Molecular Biology for Skin Diseases and STIs, Institute of Dermatology, Chinese Academy of Medical Sciences and Peking Union Medical College, Nanjing, China

Introduction

Systemic lupus erythematosus (SLE) is a prototypical autoimmune disease that is distinguished by the production of a broad spectrum of autoantibodies. Autoantibodies and antigens combine to form immune complexes (ICs), triggering complement activation and resulting in organ and tissue injury, particularly affecting the skin and kidneys [1]. In the germinal centers (GCs), B cells undergo somatic hypermutation in the variable regions of immunoglobulin genes, enabling the survival and differentiation of B cells with high-affinity antigen receptors into long-lived memory B cells and plasma cells [2]. Follicular helper T (Tfh) cells, a subtype of T helper cells (Th), are crucial for the activation and differentiation of B cells within GCs, a process that is vital for the establishment of GCs and the selection of B cells with high-affinity antigen receptors [3]. Furthermore, Tfh cells are pivotal in driving B cell responses that are T cell-dependent, particularly in the production of pathogenic autoantibodies [4]. According to research conducted on both animals and humans, the prevention of Tfh cell development may be advantageous in the treatment of lupus, rendering Tfh cells an option for drug discovery [5].

Senescence is a cellular state wherein cells irreversibly cease division and transition into a permanent growth-arrested phase, yet remain metabolically active without undergoing apoptosis [6]. This phenomenon is frequently induced by unresolved DNA damage or persistent cellular stress [7]. Cellular senescence not only contributes to the physical manifestations of aging but also initiates the process of immunosenescence [8]. It has been reported that immune function peaks during puberty but gradually declines with age, leading to the onset of immunosenescence [9]. Elderly individuals are more prone to acquiring autoimmune diseases due to weakened immune function and increased secretion of autoantibodies [10]. Furthermore, when cells age, a phenomenon known as senescence-associated secretory phenotype (SASP) occurs, in which a significant amount of cytokines, growth hormones, proteins, enzymes, and other physiologically active molecules are released. The generation of SASP relative molecules has the potential to cause persistent inflammation [11]. Therefore, the emergence of immunosenescence and chronic inflammation typifies immune dysfunction in both SLE patients and older adults [12–14]. It has been reported that anti-cellular senescence can alleviate and improve symptoms in autoimmune diseases [15, 16].

Since ancient times, humans have been aware of the medicinal properties of different phytochemicals, including their antioxidant, anti-inflammatory, antibacterial, and anticancer activities. Fruits and vegetables include flavonoids, which are secondary metabolites known for their medicinal properties. Approximately 9,000 flavonoids have been identified in natural foods so far [17, 18]. Quercetin (QC), a dietary flavonoid with promising pharmaceutical applications, has garnered increasing attention for its multifaceted medical benefits. Alongside its well-documented immune-regulating properties, QC is recognized for its antioxidative, anti-inflammatory, and anti-cancer attributes in various researches [19]. QC is commonly found in everyday foods such as fruits and vegetables, where it exists as a subtype conjugated with alcohols and sugars [20]. These subtypes are broken down in the intestines, absorbed, and metabolized into QC and other related compounds [21]. Numerous research reports suggest that QC may be effective in treating autoimmune diseases, like rheumatoid arthritis, and systemic sclerosis, among others [22].

The anti-inflammatory and pro-apoptotic properties of QC have been the subject of extensive investigation; however, the precise manner in which QC ameliorates lupus and the underlying molecular pathways remain enigmatic. Specifically, the role of QC in modulating Tfh cell function remains to be fully elucidated. The present study is designed to ascertain whether QC can inhibit the development of Tfh cells in MRL/lpr mice and exert anti-senescence effects. Additionally, this research endeavors to decipher the potential mechanisms of action, thereby enhancing the therapeutic application of QC in the management of SLE.

Methods

Reagent preparation

Sigma-Aldrich (St. Louis, MO, USA) provided the QC powder (catalogue number 6151-25-3), which was prepared as a 200 mM stock solution in dimethyl sulfoxide (DMSO). For in vitro experiments, the solution was diluted to the required final concentration in the culture medium, with DMSO serving as the control vehicle.

Animal study

As a model for spontaneous SLE, the MRL/lpr mice exhibit lupus manifestations akin to those in humans, including erythema and nephritis with proteinuria [23–25]. Female MRL/lpr mice, aged eight weeks, were procured from Spife (Beijing) Biotechnology Co, Ltd. (Beijing, China). These animals were randomly allocated into two groups: a control group and a QC treatment group, with five mice in each group. The QC stock solution was diluted in a 1% sodium carboxymethyl cellulose vehicle to yield a final suspension concentration of 15 mg/ml. The control group received daily oral gavage of the vehicle alone, whereas the QC treatment group was administered 50 mg/kg of QC via oral gavage. The weight of the mice was monitored, and their general health was assessed on a weekly basis throughout the four-month duration of the experiment. Following the experimental

period, mice were humanely euthanized by cervical dislocation. The spleen, kidneys, and mLNs were excised and weighed, and serum was collected from each mouse. All experimental procedures were conducted in accordance with the ethical guidelines approved by the Ethics Committee of the Laboratory Animal Society at Central South University (LAC-2016-0215).

Basic parameters of healthy donors

At the Health Management Center of the Second Xiangya Hospital, Central South University, peripheral blood was taken from 14 individuals in good health (refer to Supplement Table 1). All research involving human samples was conducted with the approval of the Ethics Committee of the Second Xiangya Hospital, Central South University (No. 2019044).

Enzyme-linked immunosorbent assay

Serum was collected from MRL/lpr mice at different stages of development: 12, 15, 22, 25, and 27 weeks. The serum was subjected to an overnight incubation with a cocktail of antibodies, including those directed against Total IgG (at a 1:250 dilution), dsDNA (at a 1:100 dilution), and ANA (at a 1:100 dilution) (Cusabio), to promote antibody coating on the well plates. On the subsequent day, the antibody-coated well plates were sealed, thoroughly washed, and then treated with appropriately diluted serum samples for the incubation of both primary and secondary antibodies. Following this step, the optical density (OD) readings were obtained from the microplate using a spectrophotometer set at a single wavelength of 450 nm.

H&E staining

Kidney tissue specimens were preserved using a 4% paraformaldehyde fixative. Subsequently, these samples were entrusted to Servicebio (Wuhan, China) for a series of histological procedures, including precision paraffin embedding and high-quality hematoxylin-eosin (H&E) staining to facilitate microscopic examination.

Immunofluorescence staining

The paraffin sections were deparaffinized and repaired by alkaline treatment. Primary antibodies, anti-C3 (ab20099, Abcam) and anti-IgG (ab205724, Abcam), anti-CD4 (ab183685, Abcam), anti-CD19 (ab245235, Abcam), were utilized to stain kidney sections. Opal fluorophores were then applied to the monolayer cell sections, with DAPI aiding in clarifying cell nuclei locations. The kidney sections were then scanned by multispectral imaging system (PerkinElmer Vectra).

QC effect on tfh cells in vitro

Peripheral blood mononuclear cells (PBMCs) were isolated from healthy individuals using Ficoll (GE Healthcare, cat. 17-5442-03). Subsequently, naive $CD4^+$ T cells were purified using a cell isolation kit (Miltenyi Biotec, cat. 130-050-301). Each well in a 24-well plate held 1×10^6 cells. Whereas the control group received solvent (DMSO), the experimental group received QC (dissolved in DMSO). To both groups were added the cytokines IL12, IL21, TGF-β, and IL6. After 72 h of cell incubation, flow cytometry (FCM) was employed to assess T-cell subsets and the frequency of $CD57^+$ T cells.

Flow cytometry (FCM)

Approximately 1×10^6 lymphocytes derived from mice or humans were resuspended in phosphate-buffered saline (PBS) and incubated with a panel of antibodies targeting membrane markers (refer to Supplemental Table 2) for 45 min at 4 °C in the absence of light. Following this incubation, the cells were subjected to 1 h treatment with cell membrane lysates, during which the cell membranes were permeabilized, releasing the intracellular contents. The resultant cell suspension post-rupture was then subjected to staining procedures. The prepared samples were analyzed using a BD FACSCantoTM II flow cytometer after thorough washing with PBS to remove unbound antibodies,

Reverse transcription-quantitative PCR

We used TRIzol (AG21102, AG) to extract total RNA from cells for RT-qPCR assessment of the mRNA expression of *BCL-6*, *BIM*, *IL-2*, *IL-6*, *PPARG*, *SESN3*, *CAMK4*, *PRKAG2*, *SESN1*, and *SOD2*. These primer sequences are available in the Supplementary Table 3. The kit (AG11728, AG) was then used to reverse-transcribe the RNA to cDNA. The qPCR kit (AG11740, AG) was then used to perform qPCR in a 96-well plate using a Bio-Rad CFX96 Touch system. GAPDH was used as the housekeeping gene to normalize the expression levels of target genes. RT-qPCR products' relative expression was ascertained through the application of the ΔΔ threshold cycle (CT) method. Each RT-qPCR result was subjected to three biological replicates.

RNA-sequencing analysis

The RNA-seq dataset was meticulously generated by the renowned Novogene Bioinformatics Technology Company. Our experimental protocol commenced with the selective amplification of cDNA fragments within the size range of 370 to 420 base pairs to assemble the sequencing library. Following a rigorous quality assessment to ensure the library met the required standards, we proceeded with high-throughput Illumina sequencing. Post-sequencing, we applied HISAT2 version 2.0.5

for the construction of the reference genome, having first implemented stringent data quality control measures. The expression levels of genes were quantified using the FPKM (Fragments Per Kilobase of transcript per Million mapped reads) method, which normalizes for gene length.For the identification of differentially expressed genes, we utilized the DESeq2 package within the R programming environment. Genes were deemed differentially expressed if they exhibited a p-value of less than 0.05. To gain insights into the biological significance of these differential genes, we employed clusterProfiler version 3.8.1 to conduct both Gene Ontology (GO) and Kyoto Encyclopedia of Genes and Genomes (KEGG) pathway enrichment analyses.

Cell viability assay

To investigate the cytotoxicity of QC within working concentrations, we treated PBMCs isolated from four healthy donors with QC at final concentrations of 3 and 7μM, along with a control group (0 μM, solvent). After a 3-day stimulation period, the cells were harvested and incubated with the Cell Counting Kit-8 reagent (Merck, cat. 96992-100TESTS-F). Subsequently, the cytotoxicity of the drugs was assessed by using a microplate reader (wave length 450 nm).

Cell apoptosis analysis

In a 24-well culture plate, each well was seeded with approximately 1×10^6 cells, which were subsequently cultured in an incubator set to 37 °C and 5% CO_2. The cultures were treated with varying concentrations of QC, namely 0, 5, and 7μM. On the third day of culture, the cells were harvested and stained for 20 min at room temperature in the dark, utilizing 5 μl of Annexin V-FITC and 10μL of propidium iodide. Following staining, the cells were analyzed by FCM.

Cell cycle analysis

Each well of a 24-well culture plate contained about 1×10^6 cells, which were subsequently incubated at 37 °C and 5% CO_2 in the presence of QC at concentrations of 0, 5, and 7μM. By the third day, the cells were separated by centrifugation and stored for 30 min at 4 °C in a 70% ethanol solution. Following fixation, the cells were processed using the Cell Cycle and Apoptosis Analysis Kit (Beyotime) and subsequently washed with PBS. The prepared samples were then analyzed using FCM.

Proteome microarray assays

QC-interacting proteins were found using HuProtTM Human Proteome Microarrays v4.0 (CDI Laboratories, Baltimore, MD). Microarrays were incubated with 10μM QC and D-biotin after being blocked with blocking solution. Following washing, the cells were scanned using a core LuxScan 10 K microarray chip scanner (LuxscanTM 10 K-A CapitalBio) and treated with Cy5-SA (1:1000) in the absence of light. The analysis logic was as follows: (1) For any protein, the normalized SNR value was used as the object of calculation, and the potential positive proteins were screened by cutoff threshold setting. The SNR ≥ 2 (95% confidence interval) of the standardized samples was defined as positive protein bound by QC. (2) Due to systemic reasons, there were some false positives in the screened positive proteins. In order to determine the specific binding target proteins, D-biotin was used as the control for screening positive proteins, and the SNR of standardized D-biotin < 2 was defined as the specific binding target protein of QC. Based on the above analysis logic, a total of 345 potential positive proteins for QC binding were screened, and 193 target proteins specifically binding to QC were screened using D-biotin as a control.

Statistics

This research is based entirely on statistical analysis using SPSS 20.0. Data are presented as mean values ± SEM for comparative purposes across groups. For pairwise comparisons, an unpaired, two-tailed Student's t-test was utilized. When assessing differences among more than two groups, we applied a one-way analysis of variance (ANOVA). In instances where data deviated from a normal distribution or exhibited unequal variances, the two-tailed Mann–Whitney U test was adopted. Correlation analyses were conducted using Pearson's r test for normally distributed data and Spearman's r test for data with non-normal distributions. Statistical significance was denoted by $*P<0.05$ *and* $**P<0.01$, indicating the strength of the associations observed.

Results

QC conferred a protective effect on renal damage in lupus-like mice

At 12 weeks, MRL/lpr mice were randomly assigned to the control group and QC group. Throughout the treatment regimen, all MRL/lpr mice underwent regular monitoring for survival rates, body weight variations, and fluctuations in urine protein levels (Fig. 1A). The results of the investigation showed that no discernible change in body weight was observed for either group of MRL/lpr mice over the course of the treatment (Fig. 1B). However, the QC group exhibited substantially lower urine protein levels compared to the control group after 12 and 15 weeks of treatment (Fig. 1C).

After 15 weeks of treatment, the control group had significantly greater glomerular volume, mesangial cell proliferation, and inflammatory cell infiltration than the QC group (Fig. 1D). Three kidney sections were taken from each mouse, and the mean glomerular diameter of

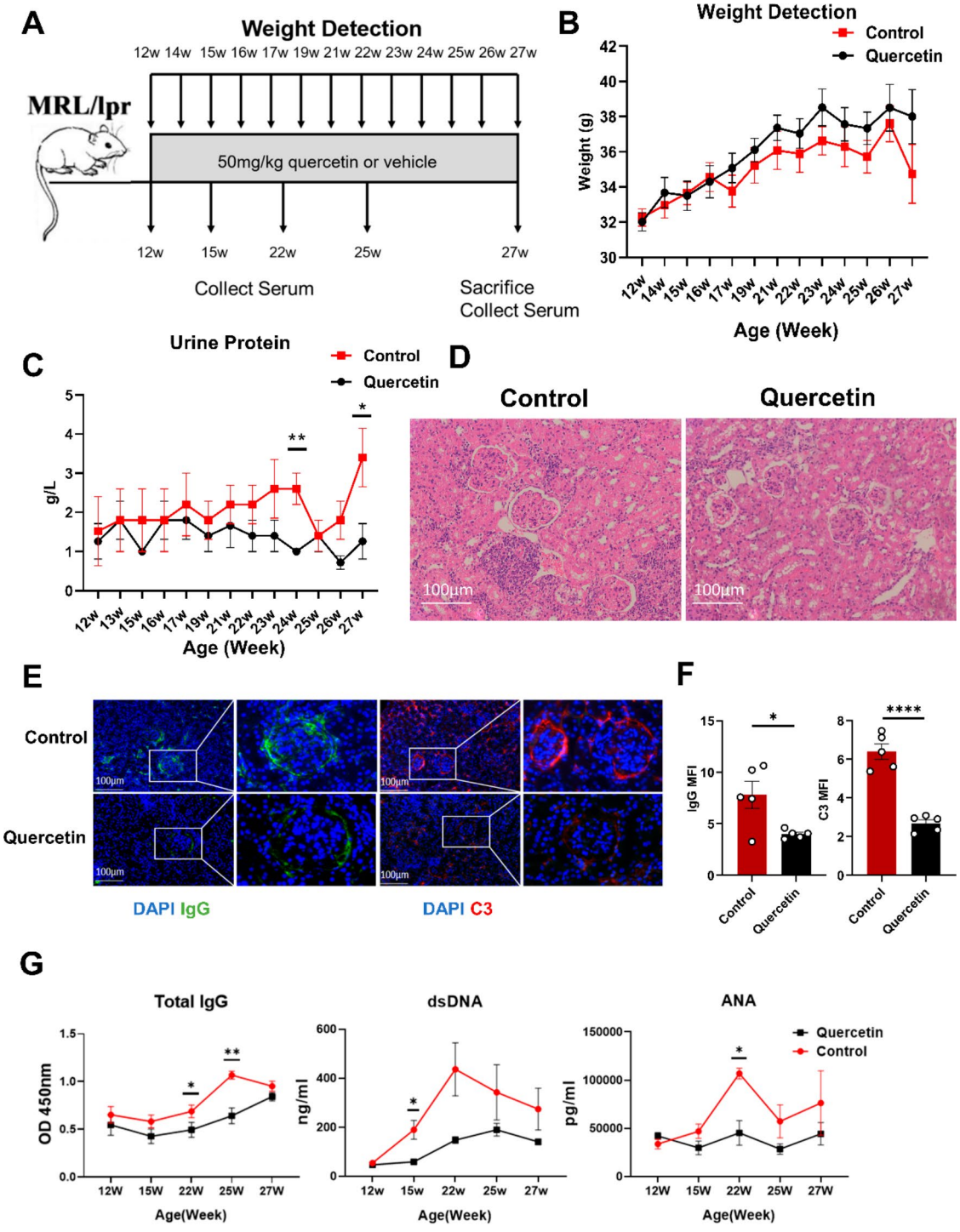

Fig. 1 QC alleviated renal damage in lupus-like mice. **(A)** Schematics for the experimental workflow with MRL/lpr lupus mice. **(B)** MRL/lpr lupus mice weight in the QC and control groups. **(C)** Urine protein changes in the MRL/lpr lupus mice treated for 15 weeks, both in the QC group and the control group. **(D)** Renal pathological changes from MRL/lpr lupus mice (200-fold field of view; H&E staining). **(E)** Immune complex deposition in the kidney of lupus-like mice, IgG shown in green, C3 shown in red, nuclei shown in blue (200-fold field of view). **(F)** Statistical analysis of mean fluorescence intensity of IgG and C3 in glomeruli. **(G)** Serum total IgG levels, Serum ANA levels and serum dsDNA levels in lupus-like mice. (Quercetin: $n = 5$, Control: $n = 5$),(*$P < 0.05$, **$P < 0.01$, ****$P < 0.0001$)

these sections was calculated to represent the glomerular diameter of that particular mouse. After QC administration, a significant reduction in glomerular diameter was observed in mice as compared with controls (Figure S1A). Subsequently, we used multispectral immunohistochemical staining to examine IgG and C3 deposition within the glomerulus (Fig. 1E). We counted the mean fluorescence intensity (MFI) of C3 and IgG in glomeruli and found that the MFI of C3 and IgG decreased significantly in the quercetin group (Fig. 1F). Furthermore, we assessed the immune cell infiltration within the kidneys and discovered that the infiltration of both T cells and B cells was substantially diminished following treatment with quercetin (Figure S1B and S1C).

MRL/lpr mice were consistently administered QC or a control treatment, and serum samples were regularly collected. Subsequently, we observed that following QC treatment, the control mice exhibited a marked reduction in total IgG levels at 22 and 25 weeks, dsDNA levels at 15 weeks, and ANA levels at 22 weeks. (Fig. 1G).

QC significantly diminished the prevalence of Tfh cells and senescent T cells within the mLNs of lupus-like mice

At the treatment endpoint, there was no differences in the weights of mLNs or spleen between the two groups were observed (Fig. 2A). Nevertheless, a notable reduction in lymphocyte count was observed in the mLNs of the QC-treated group compared to the control (Fig. 2B).

In both the mLNs and spleen of MRL/lpr mice, we conducted an investigation into the effects of QC on Tfh cells, plasma cells and senescent $CD4^+$ T cells by FCM, according to previously reported biomarkers [23–25]. We analyzed the frequencies of $CD4^+PD^-1^+CXCR5^+$ Tfh cells, $CD4^+CD44^{hi}CD62L^-PD\text{-}1^+CD153^+$ senescent $CD4^+$ T cells, and $B220^-CD138^+$ plasma cells in both the mLNs and spleens of MRL/lpr mice. The results showed that there was no significant difference in the frequency of Tfh cells (Fig. 2C and Figure S2C), senescent $CD4^+$T cells (Fig. 2D and Figure S2D) and plasma cells (Figures S2A and S2E) between the two groups. Furthermore, we determined the absolute counts of these cellular subsets and observed that quercetin treatment significantly diminished the numbers of Tfh cells (Fig. 2E), senescent $CD4^+$ T cells (Fig. 2F), and plasma cells (Figure S2B) in the mLNs.

QC exerted a statistically significant reduction in the percentage of tfh cells in vitro

To assess the impact of QC on human Tfh cells, we cultured $CD4^+$ T cells obtained from healthy individuals in the presence of QC at final concentrations of 0, 5, and 7μM for a duration of 72 h in vitro. Subsequently, the cells were harvested and subjected to FCM to quantify the percentage of Tfh and $CD4^+CD25^+CD127^-$ regulatory T (Treg) cells within the $CD4^+$ T population(Figure S3A), according to previously reported biomarkers [23, 26].

The data revealed that the presence of QC at concentrations of 5μM and 7μM led to a significant decrease in the proportion of Tfh cells within the $CD4^+$ T cell population (Fig. 3A). Furthermore, the 5μM QC treatment group displayed a statistically significant increase in the proportion of Treg cells when compared to the control group (0μM). However, no significant difference was observed in the percentage of Treg cells between the 7μM QC treatment group and the control group (Fig. 3B).

To explore the potential of QC therapy in inhibiting the progression of Tfh cell development, we conducted an experiment in which naïve $CD4^+$ T cells from healthy individuals were cultured in the presence of QC at final concentrations of 0, 5, and 7μM, along with the cytokines IL12, IL21, TGF-β, and IL6, for 3 and 7 days. The cells were subsequently harvested and the proportions of Tfh and senescent Tfh cells were measured by FCM. The results indicated that after 3 days of treatment with 7μM QC, there was a substantial reduction in the number of Tfh cells compared to the control group. Moreover, a dose-dependent decrease in the proportion of Tfh cells was observed over the course of 3 and 7 days of QC treatment (Fig. 3C).

CD57 has been identified as a specific surface marker that is expressed on senescent $CD4^+$ T cells in humans [27]. Our findings revealed a significant decrease in the percentage of senescent Tfh cells in the 7μM QC group on Day 7 compared to the control group. Besides, the 7μM QC group exhibited a greater reduction in the proportion of senescent Tfh cells after 7 days of treatment, in comparison to the 5μM QC treatment group (Fig. 3D).

QC induced apoptosis in Tfh cells in vitro

To assess the effects of QC on apoptosis, cellular samples were harvested and subjected to FCM to quantify the apoptotic index. The results indicated that exposure of $CD4^+$ T cells to 5 and 7μM QC for 3 days did not result in any alteration in the percentage of apoptotic cells when compared to the control group. However, the proportion of viable Tfh cells was notably reduced in the 7μM QC group after 3 days, as compared to the control group. Moreover, the 7μM QC group exhibited a significant decrease in viable Tfh cells compared to the 5μM QC group (Fig. 4A). Furthermore, we cultured PBMC from healthy donor with QC at a final concentration of 0, 5, and 7μM for 3 days, and then collected these cells to test the cell cytotoxicity by a CCK8 kit. The findings suggested that QC at doses of 5μM and 7μM did not exert cytotoxic effects on cell viability in comparison to the control group (Fig. 4B).

To elucidate the impact of QC within its therapeutic range on the cell cycle progression, $CD4^+$ T cells were

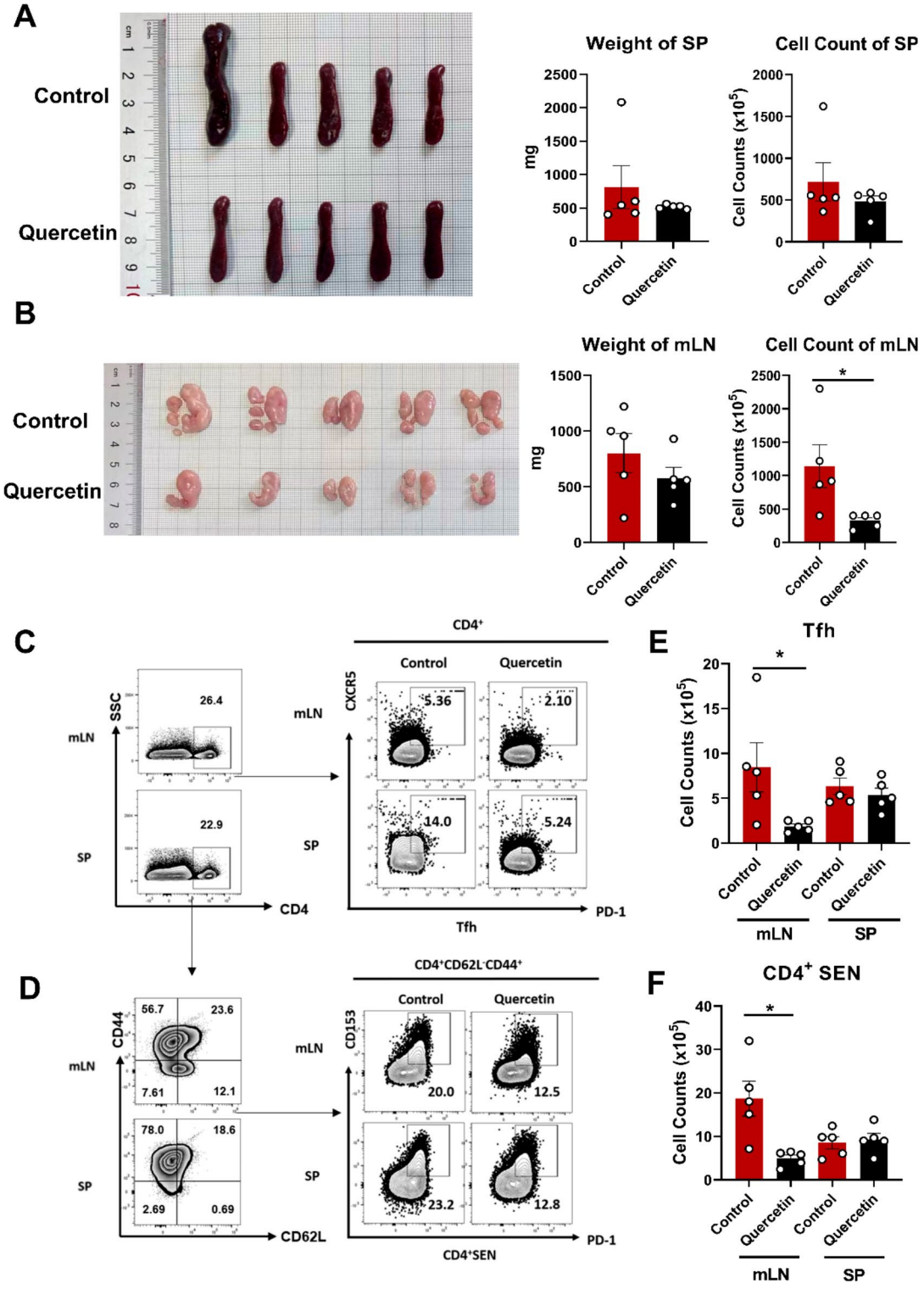

Fig. 2 QC alleviated the swelling of the mLNs s in lupus-like mice. After 15 weeks of treatment, **(A)** Spleen size and statistical analysis of spleen of weight and cell counts from MRL/lpr mice in QC group and control group. **(B)** The weight and lymphocyte cell counts of mLNs from MRL/lpr mice in the QC group and control group were statistically analysed. **(C, D)** Representative flow diagrams of the frequency of Tfh cells and senescent $CD4^+$ T cells from the spleen and mLNs of MRL/lpr mice with QC or vehicle. **(E, F)** Statistical analysis of cell counts of Tfh ($CD4^+PD^-1^+CXCR5^+$) and senescent $CD4^+$ T cells ($CD4^+CD44^{hi}CD62L^-PD\text{-}1^+CD153^+$) from the mLNs and spleen of MRL/lpr mice. (Quercetin: $n = 5$, Control: $n = 5$, $^*P < 0.05$)

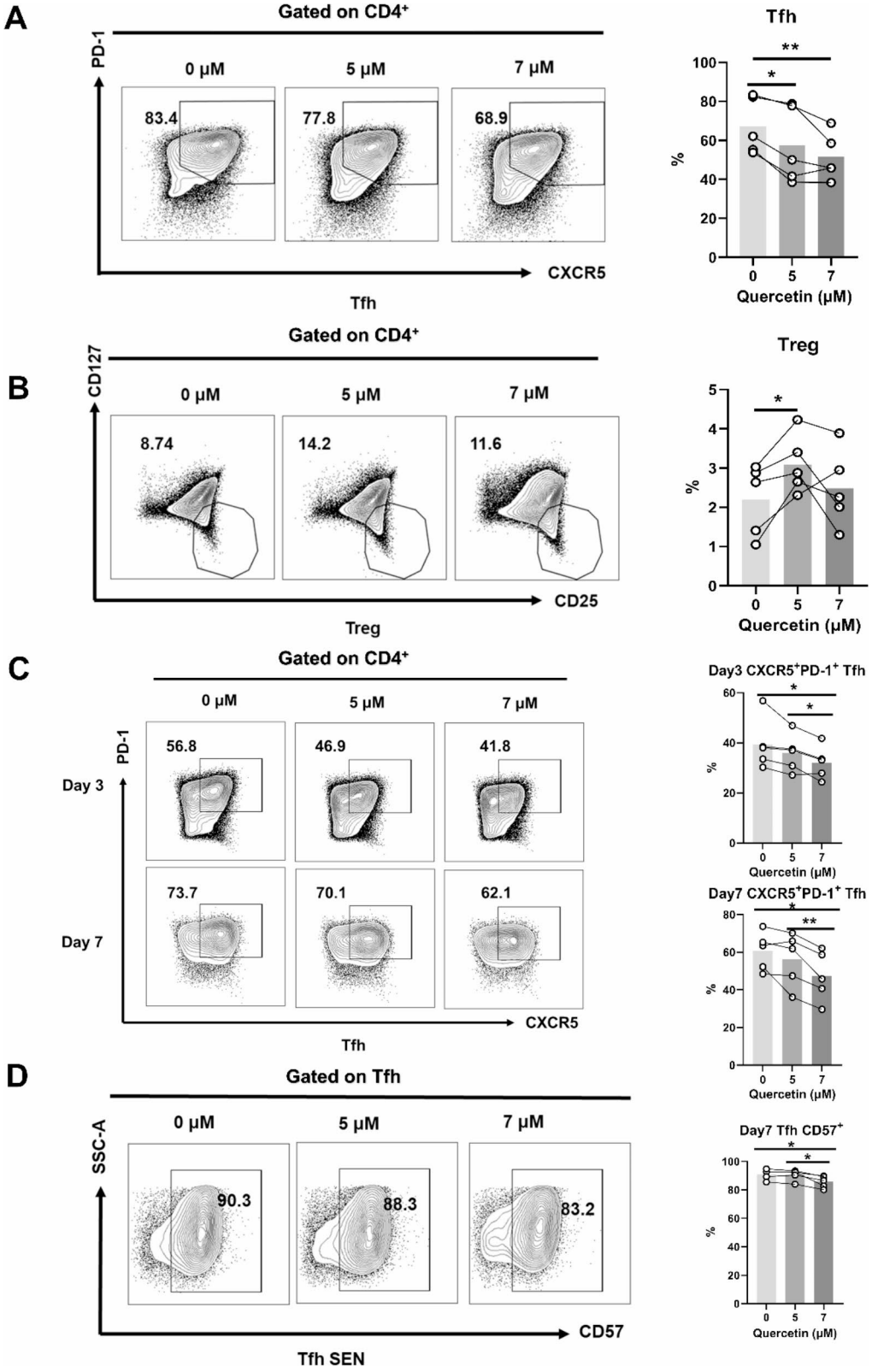

Fig. 3 QC exerted a suppressive effect on the differentiation of Tfh cells in vitro. **(A)** Quantification of the impact of various concentrations of QC on the proportion of Tfh cells by FCM. **(B)** Quantification of the impact of various concentrations of QC on the proportion of Treg cells by FCM. **(C)** Quantification of the impact of various concentrations of QC on Tfh cell differentiation on day 3 and day 7 by FCM ($n = 5$). **(D)** Quantification of the impact of various concentrations of QC on the proportion of senescent Tfh cells on day 7 by FCM ($n = 5$). (*$P < 0.05$, **$P < 0.01$)

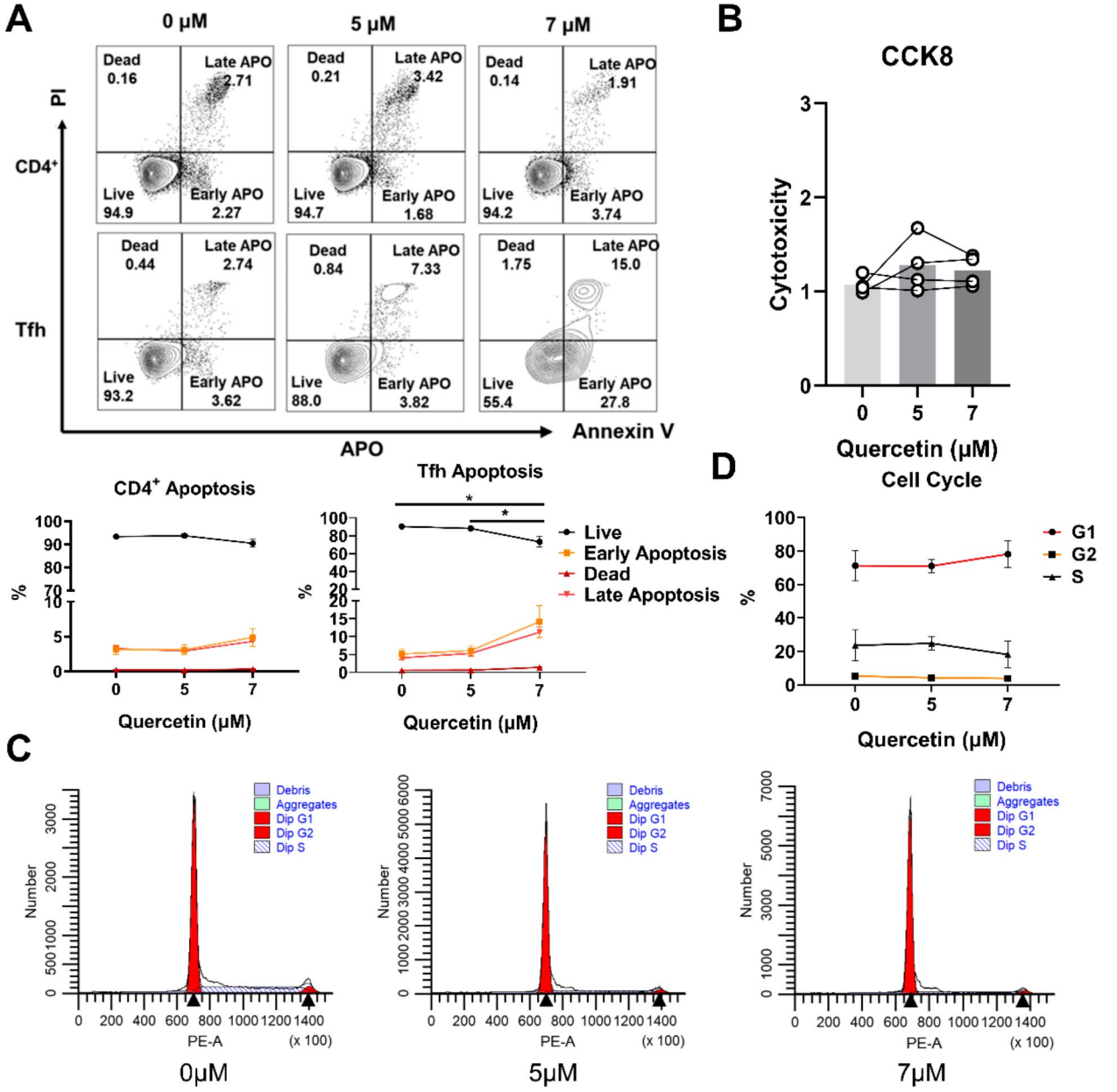

Fig. 4 QC induced apoptosis in Tfh cells in vitro.**(A)** Quantification of the effect of different levels of QC on apoptosis in $CD4^+$ T cells and Tfh cells over a 3-day period by FCM ($n=4$). **(B)** The cytotoxic effects of various concentrations of QC on PBMCs ($n=4$). **(C, D)** The impact of QC at varying concentrations on the cell cycle progression of $CD4^+$ T cells ($n=4$). (*$P<0.05$)

obtained from healthy donors cultured with QC at final concentrations of 0, 5, and 7 μM for 3 days in vitro. Subsequently, the FCM was employed to analyze the distribution of cells across each phase of the cell cycle and to investigate the influence of QC on $CD4^+$ T cell cycle dynamics (Fig. 4C). The data indicated that no significant disparities in the cell cycle were observed between the 5 μM and 7 μM QC groups and the control group (Fig. 4D).

QC induced upregulation of apoptosis-related gene expression while downregulating genes associated with Tfh cells differentiation

We conducted an RNA sequencing (RNA-seq) analysis to compare the global transcriptional profiles of $CD4^+$ T cells between the control group and the 7μM QC group on Day 3. Utilizing DESeq2 analysis in R with a significance threshold of $p<0.05$, we identified a total of 2,266 differentially expressed genes (DEGs) in the qc treatment group. This dataset comprised 973 genes that were upregulated and 1,293 genes that were downregulated

in comparison to the control group(Figure 5A). Additionally, we found that apoptosis related genes (including *BCL2L11(BIM), PIK3CB, BCL2A1, CASP3, CAPN2, TNFSF11, ACTBP2, TNFRSF10A, TNFRSF11A and ATM*) were up-regulated after QC intervention. The increased expression levels of these genes could be dominant factor to promote cell apoptosis. While the expression levels of apoptosis-resistant genes were also

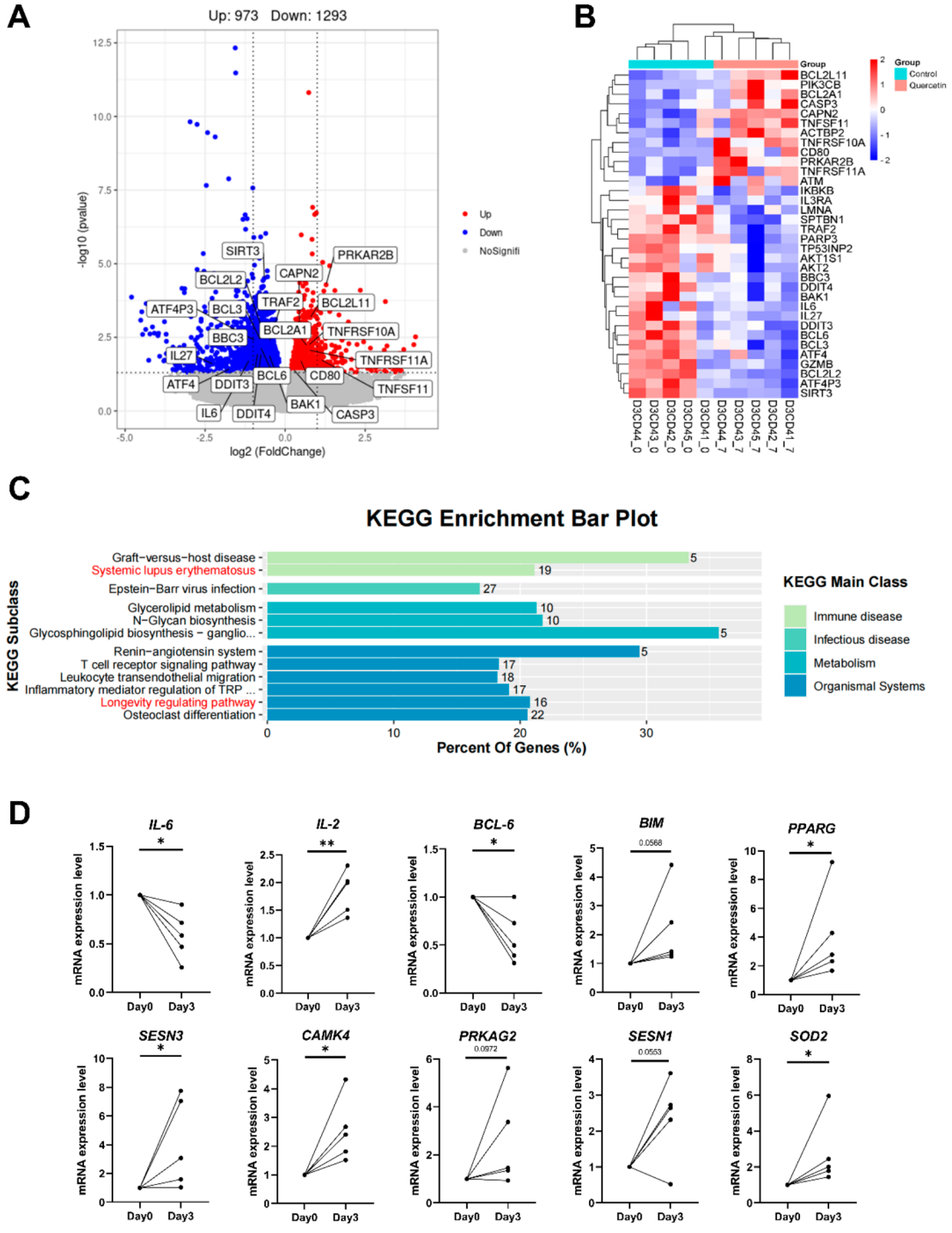

Fig. 5 QC increased apoptosis genes while suppressing Tfh cell genes. **(A)** Volcano diagram of DEGs (differentially expressed genes) of $CD4^+$ T cells between control group and QC group ($n=5$). **(B)** Heatmap of DEGs related to apoptosis, senescence and differentiation in control group and QC group ($n=5$). **(C)** KEGG enrichment analysis of $CD4^+$ T cells in control group and QC group ($n=5$), these pathways were significant differences in the diagram. **(D)** RT-PCR verified relative expression of mRNA in control group and QC group, Values are shown as mean ± SEM ($n=5$, $^*P<0.05$, $^{**}P<0.01$)

decreased, such as *IKBKB*, *IL3RA*, *LMNA*, *SPTBN1*, *TRAF2*, *RARP3*, *TP53INP2*, *AKT2*, *AKT1S1*, *BBC3*, *DDIT4*, *BAK1*, *BCL3*, *ATF4*, *GZMB*, *BCL2L2*, *ATP4P3 and SIRT3*(Fig. 5B). This maybe indicate that QC could attenuate cell senescence by promoting cell apoptosis.

KEGG pathway analysis identified the predominant enrichment pathways as "Systemic lupus erythematosus", "the Longevity regulating pathway", and other immune-related pathways, which indicated that QC ameliorates lupus symptoms probably by regulating immune and inflammatory homeostasis.

Subsequently, we identified a downregulation of key gene including *IL6*, *IL21-AS1*, *IL27*, and *BCL6*, and an upregulation of *FOXP1* and *CD80*, as revealed by RNA-seq analysis. These cytokines and transcription factors are pivotal in the differentiation of Tfh cells, suggesting that QC may interfere with Tfh cell differentiation by modulating cytokine and transcription factors expression. To corroborate these findings, we employed RT-qPCR to validate the mRNA expression levels of Tfh cell-associated molecule. The RT-qPCR results revealed an increase in *IL2* mRNA expression in the QC group compared to the control group, while *BCL6* and *IL6* expression levels were observed to decrease, aligning with the RNA-seq data. Moreover, we detected a significant upregulation of genes associated with "the longevity regulating pathway", such as *PPARG*, *SESN3*, *CAMK4*, and *SOD2*, in the QC group (Fig. 5D). These observations collectively indicate that QC may inhibit Tfh cell differentiation by promoting the apoptosis of senescent cells.

Identification of BCL-2 as a direct QC-Binding protein

To reveal the underlying mechanisms by which QC regulates cellular senescence gene expression, we screened for potential QC-binding proteins. We assessed the binding of QC to recombinant proteins synthesized on a HuProt human protein microarray. After incubation with QC or D-biotin, binding was detected using Cy5-SA (Cy5-streptavidin). (Fig. 6A). Additionally, we screened 193 target proteins for QC-specific binding using D-biotin as a control, further these specific positive proteins were used to construct protein-protein interactions (Fig. 6B). BCL-2, CASP8, MAPK8 were the main targets of the PPI network.

Using the KEGG database, we conducted pathway enrichment analysis on the 193 sample-specific binding target proteins (Supplementary Material 1). We identified BCL-2-related pathways that had a p-value less than 0.05 and used them to create the bar map. The KEGG pathways analysis revealed that the main enrichment pathway included the "Apoptosis", "Endocrine resistance" and "Necroptosis" (Fig. 6C).

A bar chart was plotted to show the BCL-2 related terms with a p-value < 0.05 for each of the three functional modules in the enrichment analysis of 193 samples that specifically bind to target proteins based on the Gene Ontology database. The GO enrichment analysis indicate that QC exerts its biological effects through "cellular response to oxidative stress", "focal adhesion assembly", "neural nucleus development" and other biological processes and molecular functions (Fig. 6D). The Protein-Protein Interaction Networks analysis revealed that QC interacts with BCL-2 family protein.

Discussion

MRL/lpr mice are currently a highly prevalent animal model for SLE. Studies have shown that there are senescent bone marrow mesenchymal stem cells, senescent nerve cells, senescent kidney cells and senescent immune cells in lupus model mice [28–31]. Notably, senescent immune cells, particularly senescent $CD4^+$ T cells, significantly contribute to the enhancement of antibody production by B cells, and they are crucial in the development of SLE [29]. Various autoantibodies and inflammation are pathological features of SLE. The pathogenesis of lupus involves a multitude of factors, with genetics and infection being considered as the primary contributors. Recently, various researchers have noted that "inflammaging," including immunosenescence and inflammation, is a common feature of the elderly and SLE patients [32].

Tfh cells are a particular type of T helper cells involved in humoral immunity which were considered to assist B cells to produce antibodies [33]. Current studies have found that Tfh cells have the capability to produce IL-21, which in turn activates $CD8^+$ T cells, thereby playing an essential role in enhancing $CD8^+$ T cell-mediated immunity [34]. In Sanroque mice, mutations in the Roquin gene result in the hyperactivation of ICOS and OX40 signaling pathways, coupled with the over-secretion of IL-21, thereby fostering the excessive proliferation of Tfh cells. Consequently, this cascade leads to the hyperactivation of germinal center B cells (GCB cells) and the excessive production of high-affinity pathogenic autoantibodies. It induces the formation of high-affinity anti-dsDNA antibodies, swell of lymph nodes and spleen, and other systemic lupus-like phenotypes [35]. Besides, the IL-2 pathway is crucial in the development of several autoimmune disorders and acts as a key controller of Tfh differentiation. Thus, the role of Tfh cells in the development of autoimmune diseases is crucial [36]. Notably, In SLE patients, Tfh cells are primarily responsible for modulating B cell activation and differentiation, promoting autoantibody production, and influencing the balance of the immune response [37]. In SLE patients, Tfh cells are primarily responsible for modulating B cell activation and differentiation, promoting autoantibody production, and influencing the balance of the immune response.

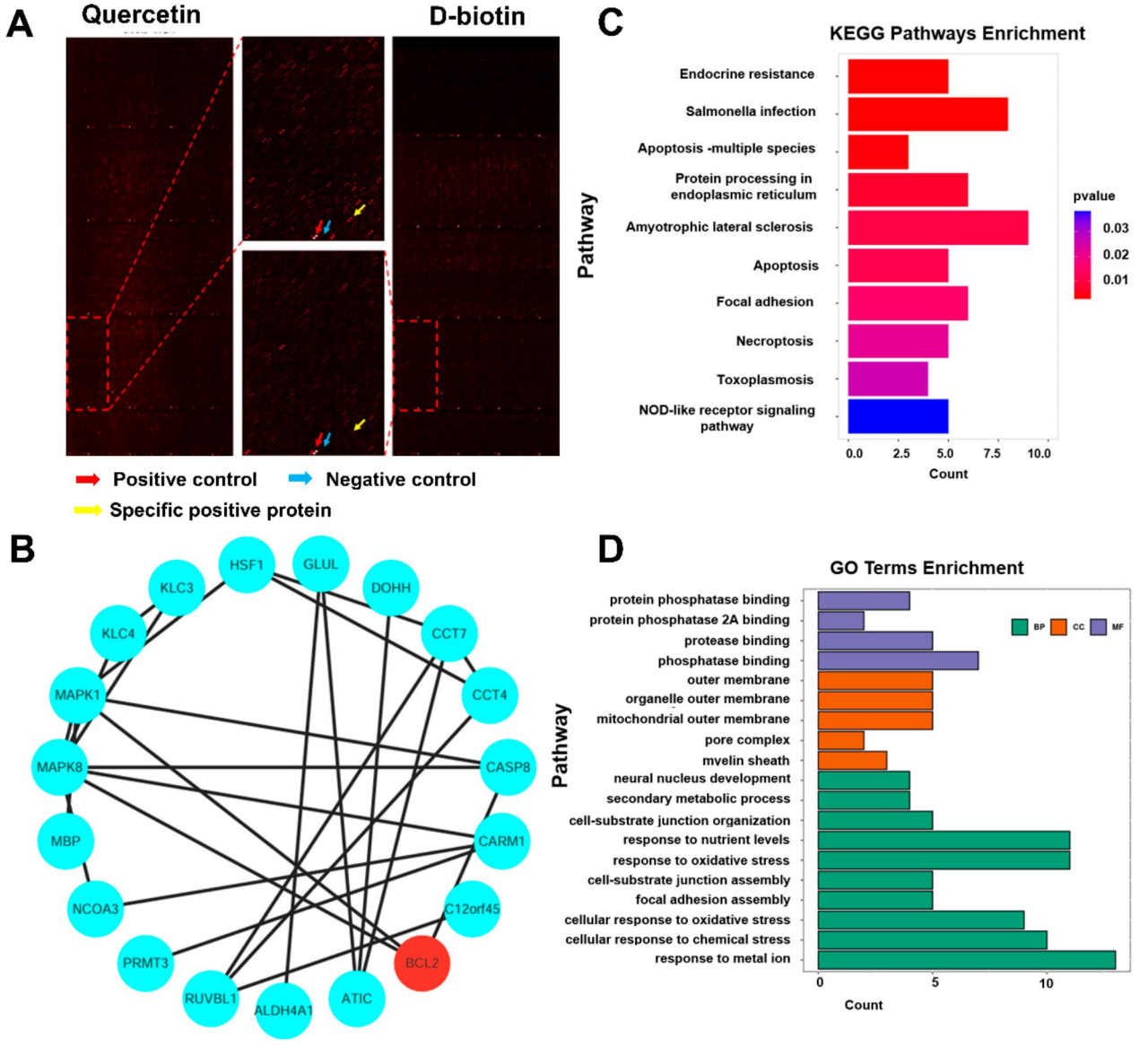

Fig. 6 Identification of QC-binding proteins. **(A)** The protein microarray representation depicts red arrows as positive points, blue arrows as negative control points, and yellow arrows as specific positive protein points. **(B)** Visualization results of the protein–protein interaction network of specific positive protein. **(C)** The KEGG pathway analysis is performed on specific positive proteins to elucidate the pathways associated with BCL-2. The bar length corresponds to the number of target genes, while the bar colors correspond to the different values of p-value. **(D)** GO functional enrichment analysis associated with BCL-2 in specific positive proteins, including biological processes (BP), molecular functions (MF), and cellular components (CC)

Significant risks to the lives of patients are posed by the anomalous activation and function of Tfh cells in SLE, which exacerbate the inflammatory response and autoantibody production [38].

Both animal experiments and human studies provide compelling evidence that inhibiting Tfh cells can offer therapeutic benefits for individuals with lupus. Tfh cells are potentially a pivotal target for the development of new medications [5]. Our research revealed an elevation in both Tfh cells and senescent T cells in the mLNs of mouse models with SLE. However, treatment with QC resulted in a decrease in the proportion of Tfh cells and senescent T cells. Through the analysis of RNA-seq data, we discovered that QC effectively inhibits the differentiation of $CD4^+$ T cells into Tfh cells by modulating the expression of cytokines and transcription factors. Specifically, QC treatment led to the downregulation of *IL-6*, *IL21-AS1*, *IL-27*, and *BCL-6*, while upregulating *FOXP1* in $CD4^+$ T cells. Notably, *BCL-6* functions as a key transcription factor that is essential for the development of Tfh cells. It plays a critical role in encouraging the differentiation of Tfh cells, activating B cells, and facilitating the establishment of germinal centers [39]. *IL-6* and *IL-27* have the ability to increase the production

of *BCL-6*, which in turn boosts the development of Tfh cells by activating transcription factors *STAT3* or *STAT4* [40]. On the other hand, *FOXP1* acts as a critical negative transcription regulator for Tfh cell differentiation. Subsequently, we validated the mRNA expression levels of Tfh cell-associated cytokines by RT-qPCR, revealing that QC treatment led to an upregulation of *IL-2* mRNA expression levels, while downregulating *IL-6* and *BCL-6*.

In addition, the result of HuProt human protein microarray shown that QC directly binds to BCL-2 family proteins, which suggested that BCL-2 are potential targets for QC action. As previously reported, BCL-2 is highly expressed in both B cells and T cells of SLE patients [16, 41, 42]. This increased expression is likely to disrupt programmed cell death, leading to lymphoid hyper-reactivity, and contributing to the initiation and perpetuation of this archetypal systemic autoimmune condition. A study has reported that BCL-2 inhibitor ABT-263 can effectively alleviate the lupus-like phenotype of MRL/lpr mice, as shown by decreased serum antinuclear antibody levels, decreased urinary protein levels, and improved renal pathology [43].

Our research suggests that QC demonstrated potential in reducing symptoms of lupus both in vitro and in vivo. Notably, QC was observed to decrease urine protein levels, mitigate the pathological progression of kidney damage, alleviate swelling in mLNs and spleen in lupus mice, and reduce the populations of Tfh cells, PC cells, and senescent $CD4^+$ T cells in mLNs. Similarly, in vitro experiments also revealed that QC can inhibit Tfh cells differentiation and encourage senescent Tfh cells apoptosis without causing cytotoxic effects. These findings from our study may inspire innovative strategies utilizing QC to target Tfh cells and enhance the effectiveness of SLE treatment.

Conclusion

In summary, our findings demonstrate that QC effectively reduces urine protein levels, alleviates lymph node swelling, and ameliorates the pathological deterioration in the kidneys of MRL/lpr lupus mice. Moreover, our research revealed that QC effectively inhibits the differentiation of $CD4^+$ T cells into Tfh cells by modulating the expression of cytokines and transcription factors. while also down-regulating immunosenescence by promoting the apoptosis of senescent Tfh cells through the BCL-2 pathway. In conclusion, our findings highlight the potential of QC to inhibit Tfh cell differentiation and mitigate Tfh cell immunosenescence, positioning it as a promising therapeutic strategy for treating SLE.

Abbreviations

SLE	Systemic lupus erythematosus
QC	Quercetin
IC	Immune complex
mLN	Mesenteric lymph node
Tfh	Follicular helper T
GC	Germinal center
Th	T helper cells
SASP	Senescence-associated secretory phenotype
DMSO	Dimethyl sulfoxide
FCM	Flow cytometry
PBS	Phosphate-buffered saline
MFI	Mean fluorescence intensity
GO	Gene Ontology
KEGG	Kyoto Encyclopedia of Genes and Genomes
SEN	Senescent
Treg	Regulatory T
APO	Apoptosis
DEG	Differentially expressed gene

Supplementary Information

The online version contains supplementary material available at https://doi.org/10.1186/s12979-024-00474-9.

Supplementary Table

Supplementary Figure

Supplementary Material 1

Acknowledgements

This work was supported by the Special Program of National Natural Science Foundation of China (No. 32141004), the National Natural Science Foundation of China (No. 82173425, No. 82373488,No. 82473530), the National Key R&D Program of China (No. 2021YFC2702004), the CAMS Innovation Fund for Medical Sciences (CIFMS) No.2021-I2M-1-059, the Non-profit Central Research Institute Fund of Chinese Academy of Medical Sciences(2020-RC320-003), Major Scientific Research Program for High-Level Health Personnel in Hunan Province Health and Family Planning Commission (No.2023041), the health research project of Hunan Provincial Health Commission of China (No. W20243055), Natural Science Foundation of Hunan Province of China (No. 2022JJ40722, No. 2024JJ4077).

Author contributions

QJ. L., HJ. W., and M. Y. designed the experiments. F. X. and K. S. wrote the manuscript. F. X. conducted the mouse model construction, PBMC experiments, and data analysis. K. S. handled data collation and analysis. D. L., SQ .Z., and Y. X. conducted the PBMC experiments. YZ.X conducted the Elisa experiments. PL. R. provided guidance on RNA-seq analysis. WJ. P. performed the microarray analysis. M. Y. provided guidance on FCM data analysis, and M. Y., HJ. W., and QJ. L. edited the manuscript. M.Y., HJ. W., and QJ. L. led the investigation, oversaw the research, and finalized the manuscript. All authors reviewed and approved the final manuscript.

Data availability

No datasets were generated or analysed during the current study.

Declarations

Competing interests

The authors declare no competing interests.

Received: 7 August 2024 / Accepted: 8 October 2024
Published online: 15 October 2024

References

1. Victora G D, Nussenzweig MC. Germinal centers. Annu Rev Immunol. 2022;40:413–42.
2. Vinuesa C G, Cyster JG. How T cells earn the follicular rite of passage. Immunity. 2011;35(5):671–80.
3. Crotty S. T follicular helper cell differentiation, function, and roles in disease. Immunity. 2014;41(4):529–42.

4. Vinuesa C G, Sanz I, Cook MC. Dysregulation of germinal centres in autoimmune disease. Nat Rev Immunol. 2009;9(12):845–57.
5. Gensous N, Schmitt N, Richez C, et al. T follicular helper cells, interleukin-21 and systemic lupus erythematosus. Rheumatology (Oxford). 2017;56(4):516–23.
6. Campisi J, D'adda Di Fagagna F. Cellular senescence: when bad things happen to good cells. Nat Rev Mol Cell Biol. 2007;8(9):729–40.
7. D'adda Di Fagagna F. Living on a break: cellular senescence as a DNA-damage response. Nat Rev Cancer. 2008;8(7):512–22.
8. Franceschi C, Monti D. Successful immunosenescence and the remodelling of immune responses with ageing. Nephrol Dial Transpl. 1996;11(Suppl 9):18–25.
9. Montoya-ortiz G. Immunosenescence, aging, and systemic lupus erythematous. Autoimmune Dis, 2013, 2013: 267078.
10. Liao S, Ning Q, Chen Y, et al. Interaction of aging and Immunosenescence: New therapeutic targets of aging. Int Immunopharmacol. 2022;113(Pt A):109397.
11. Teissier T, Boulanger E, Cox LS. Interconnections between Inflammageing and Immunosenescence during ageing. Cells, 2022, 11(3).
12. FüLöP T, Larbi A, Dupuis G, et al. Ageing, autoimmunity and arthritis: perturbations of TCR signal transduction pathways with ageing - a biochemical paradigm for the ageing immune system. Arthritis Res Ther. 2003;5(6):290–302.
13. Candore G, Caruso C. Low grade inflammation as a common pathogenetic denominator in age-related diseases: novel drug targets for anti-ageing strategies and successful ageing achievement. Curr Pharm Des. 2010; 16(6): 584–96.
14. Fulop T, Larbi A, Dupuis G, et al. Immunosenescence and Inflamm-Aging as two sides of the same Coin: friends or foes?. Front Immunol. 2017;8:1960.
15. Chen Y, Li X. A 2-week time-restricted feeding attenuates psoriasis-like lesions with reduced inflammatory cytokines and immunosenescence in mice. Exp Dermatol. 2023;32(11):2000–11.
16. Jiang J, Yang M, Zhu H et al. CD4 + CD57 + senescent T cells as promoters of systemic lupus erythematosus pathogenesis and the therapeutic potential of senolytic BCL-2 inhibitor. Eur J Immunol, 2024: e2350603.
17. Xiao Z P, Peng Z Y, Peng M J, et al. Flavonoids health benefits and their molecular mechanism. Mini Rev Med Chem. 2011;11(2):169–77.
18. Haddad A Q, Fleshner N. Antiproliferative mechanisms of the flavonoids 2,2'-dihydroxychalcone and fisetin in human prostate cancer cells. Nutr Cancer. 2010;62(5):668–81.
19. Formica JV. Review of the biology of Quercetin and related bioflavonoids. Food Chem Toxicol. 1995;33(12):1061–80.
20. Kumar S, Pandey AK. Chemistry and biological activities of flavonoids: an overview. ScientificWorldJournal, 2013, 2013: 162750.
21. Moon JH, Tsushida T, Nakahara K, et al. Identification of quercetin 3-O-beta-D-glucuronide as an antioxidative metabolite in rat plasma after oral administration of quercetin. Free Radic Biol Med. 2001;30(11):1274–85.
22. Shen P, Lin W, Deng X, et al. Potential implications of Quercetin in Autoimmune diseases. Front Immunol. 2021;12:689044.
23. Jordan-paiz A, Martrus G, Steinert F L, et al. CXCR5 + PD-1 + + CD4 + T cells colonize infant intestines early in life and promote B cell maturation. Cell Mol Immunol. 2023;20(2):201–13.
24. Sato Y, Oguchi A, Fukushima Y et al. CD153/CD30 signaling promotes age-dependent tertiary lymphoid tissue expansion and kidney injury. J Clin Invest, 2022, 132(2).
25. Krishnamurty A T, Thouvenel C D, Portugal S, et al. Somatically Hypermutated Plasmodium-Specific IgM(+) memory B cells are Rapid, Plastic, early responders upon Malaria Rechallenge. Immunity. 2016;45(2):402–14.
26. Brown M E, Peters L D, Hanbali S R, et al. Human CD4 + CD25 + CD226- Tregs demonstrate increased purity, Lineage Stability, and suppressive capacity Versus CD4 + CD25 + CD127lo/- Tregs for adoptive cell therapy. Front Immunol. 2022;13:873560.
27. Brenchley JM, Karandikar N J, Betts M R, et al. Expression of CD57 defines replicative senescence and antigen-induced apoptotic death of CD8 + T cells. Blood. 2003;101(7):2711–20.
28. Tahir S, Fukushima Y, Sakamoto K, et al. A CD153 + CD4 + T follicular cell population with cell-senescence features plays a crucial role in lupus pathogenesis via osteopontin production. J Immunol. 2015;194(12):5725–35.
29. Sakamoto K, Fukushima Y, Ito K, et al. Osteopontin in spontaneous germinal centers inhibits apoptotic cell Engulfment and Promotes Anti-nuclear antibody production in Lupus-Prone mice. J Immunol. 2016;197(6):2177–86.
30. Ji J, Fu T, Dong C, et al. Targeting HMGB1 by ethyl pyruvate ameliorates systemic lupus erythematosus and reverses the senescent phenotype of bone marrow-mesenchymal stem cells. Aging. 2019;11(13):4338–53.
31. Gu Z, Tan W. Rapamycin reverses the senescent phenotype and improves immunoregulation of mesenchymal stem cells from MRL/lpr mice and systemic lupus erythematosus patients through inhibition of the mTOR signaling pathway. Aging. 2016;8(5):1102–14.
32. Tsai C-Y, Shen C-Y, Liao H-T et al. Molecular and Cellular bases of Immunosenescence, inflammation, and Cardiovascular complications mimicking inflammaging in patients with systemic lupus erythematosus. Int J Mol Sci, 2019, 20(16).
33. CROTTY S. Follicular helper CD4 T cells (TFH). Annu Rev Immunol. 2011;29:621–63.
34. Zander R, Kasmani M Y, Chen Y et al. Tfh-cell-derived interleukin 21 sustains effector CD8 + T cell responses during chronic viral infection. Immunity, 2022, 55(3).
35. Vinuesa C G, Cook M C, Angelucci C, et al. A RING-type ubiquitin ligase family member required to repress follicular helper T cells and autoimmunity. Nature. 2005;435(7041):452–8.
36. Walker L S K. The link between circulating follicular helper T cells and autoimmunity. Nat Rev Immunol. 2022;22(9):567–75.
37. Mao M, Xu S, Lin L, et al. Impact of corticosteroids on the proportions of circulating tfh cell subsets in patients with systemic Lupus Erythematous. Front Med (Lausanne). 2022;9:949334.
38. Simpson N, Gatenby P A, Wilson A, et al. Expansion of circulating T cells resembling follicular helper T cells is a fixed phenotype that identifies a subset of severe systemic lupus erythematosus. Arthritis Rheum. 2010;62(1):234–44.
39. Liu D, Yan J, Sun J et al. BCL6 controls contact-dependent help delivery during follicular T-B cell interactions. Immunity, 2021, 54(10).
40. Gómez-MartíN D, Díaz-Zamudio M, Romo-Tena J, et al. Follicular helper T cells poise immune responses to the development of autoimmune pathology. Autoimmun Rev. 2011;10(6):325–30.
41. Liphaus B L, Kiss M H B Carrascos, et al. Increased Fas and Bcl-2 expression on peripheral mononuclear cells from patients with active juvenile-onset systemic lupus erythematosus. J Rheumatol. 2007;34(7):1580–4.
42. Gatenby P A Irvinem. The bcl-2 proto-oncogene is overexpressed in systemic lupus erythematosus. J Autoimmun. 1994;7(5):623–31.
43. Jiang J, Yang M, Zhu H, et al. CD4 + CD57 + senescent T cells as promoters of systemic lupus erythematosus pathogenesis and the therapeutic potential of senolytic BCL-2 inhibitor. Eur J Immunol. 2024;54(7):e2350603.

Publisher's note